Proceedings World Geothermal Congress 2010
Bali, Indonesia, 25-29 April 2010

Numerical Simulation of Exploitation of Supercritical Enhanced Geothermal System

Roman I. Pashkevich[1] and Vitaly V. Taskin[2]

SRGC FEB RAS, Severo-vostochnoe shosse, 30, Petropavlovsk-Kamchatsky, 683002, Russian Federation

[1]teplosnab@rambler.ru, [2]taskin-v@yandex.ru

Keywords: HDR, EGS; triplet well system, magma, supercritical; numerical modeling

ABSTRACT

The modeling of a triplet well system operation under supercritical initial conditions was performed. The distributions of temperature, pressure, and water saturation and their respective changes during exploitation were explored. The variation of heat production, bottom-hole temperature, bottom-hole pressure, and water saturation were investigated as a function of the well discharge and the mutual geometrical location of wells.

1. INTRODUCTION

Magmatic geothermal systems have recently been discussed as potential targets for development. In such systems, the supercritical fluid exists at depth at temperatures exceeding 400°C and pressures exceeding 22 MPa. The development of such systems can be realized using circulation technology called HDR/EGS technology. Few supercritical EGS simulations have been performed (Yano and Ishido, 1998, Watanabe, Niibori and Hashida, 2000, Brikowski, 2001, Croucher and O'Sullivan, 2008).

In these papers, the calculations were accomplished in a narrow range of parameters and without determination of the rational distance between injectors and producers (denoted as L in Figure 1) and relative vertical distance between the injector bottom and the producer bottom (H_r).

The response to the exploitation of a deep supercritical geothermal reservoir with an initial temperature of 375–400°C was numerically researched by Yano and Ishido (1998) using the STAR simulator (Pritchett, 1995). The operation of a single producer was simulated. Calculations were made for a short exploitation time of 0.1 year. The STAR simulator has upper parameter limits of 1000 bar and 800°C. The simulation of doublet operation (one injector and one producer) in a single fracture reservoir with 100x100x100 m dimensions and a well distance of 25 m is presented by Watanabe, Niibori and Hashida (2000). The "five-spot" (four injectors and one producer) TOUGH2 problem (Pruess, Oldenburg and Moridis, 1999) was extended to supercritical conditions with small producer rate 0.9 kg/s by Brikowski (2001). Another supercritical version of TOUGH2 was developed by Kissling and White (1999). Recently, Croucher and O'Sullivan (2008) have presented a new supercritical TOUGH2 version and compared of their results for the supercritical "five-spot" problem to the earlier studies.

The HYDROTHERM program (Hayba and Ingebritsen, 1994, Kipp, Hsieh and Charlton, 2008) correctly simulates up to 1,200°C and 1 GPa and was used in more than 30 simulations of deep hydrothermal, volcanic and magmatic geothermal systems at supercritical conditions. The Cersions 2.2 and 3.0 of HYDROTHERM were used in this paper.

A visual comparison of the results of the current HYDROTHERM ver. 3.0 simulation of the supercritical "five-spot" problem with the supercritical TOUGH2 results obtained by Brikowski, (2001) and Croucher and O'Sullivan (2008) is presented in Figure 2. In the reservoir of the Fenton Hill project (1975-1995, USA) created by subvertical fractures, the injector was 100 m deeper than the producer. In the current Soultz HDR project (Ledru, 2007) and the commercial Cooper Basin HFR project, the well pattern with H_r=0 is accepted (Vörös, Weidler and Wyborn, 2007). For the case of subcritical EGS, the influence of L on the heat mining efficiency was researched using TOUGH2 simulations by Sanyal and Butler (2005), but the role of H_r was not discussed.

2. NUMERICAL MODEL

In the present paper, the results of the numerical modeling of triplet well pattern operation (one injector and two producers, as shown in Figure 1) are discussed. The well depth of 2700 m was used, and the initial temperature and pressure at the well bottoms were 380°C and the 22.5 MPa, respectively. The injector mass rate G was varied from 5 to 15 kg/s. The value of H_r was varied from 0 to 550 m, and the value of L was varied from 200 to 500 m. The bottom-hole water temperature in the injection well was assumed to be 100°C. The well open intervals used were 50 m. The dimensions of the simulated region were 1950 m x 1000 m x 3000 m, as shown in Figure 1. The reservoir consisted of one production zone with a rock permeability of 10^{-15} m^2, a thickness of 1800 m, and two impermeable rocks (10^{-20} m^2): a 1000 m thick upper layer and a 200 m thick lower layer. The initial domain pressure was hydrostatic. On the upper boundary, a pressure of 0.1 MPa and a temperature of 10°C were assigned. The initial temperature gradient was 0.137°C/m, and the initial temperature at the bottom boundary was 420°C.

It is supposed that a productive permeable zone can be created by hydraulic fracturing. The experience of HDR/EGS creation (Future of Geothermal Energy, 2006) indicates the possibility to stimulate a large volume of permeable rocks (more than 2 km^3) at depths ranging from 3 – 5 km.

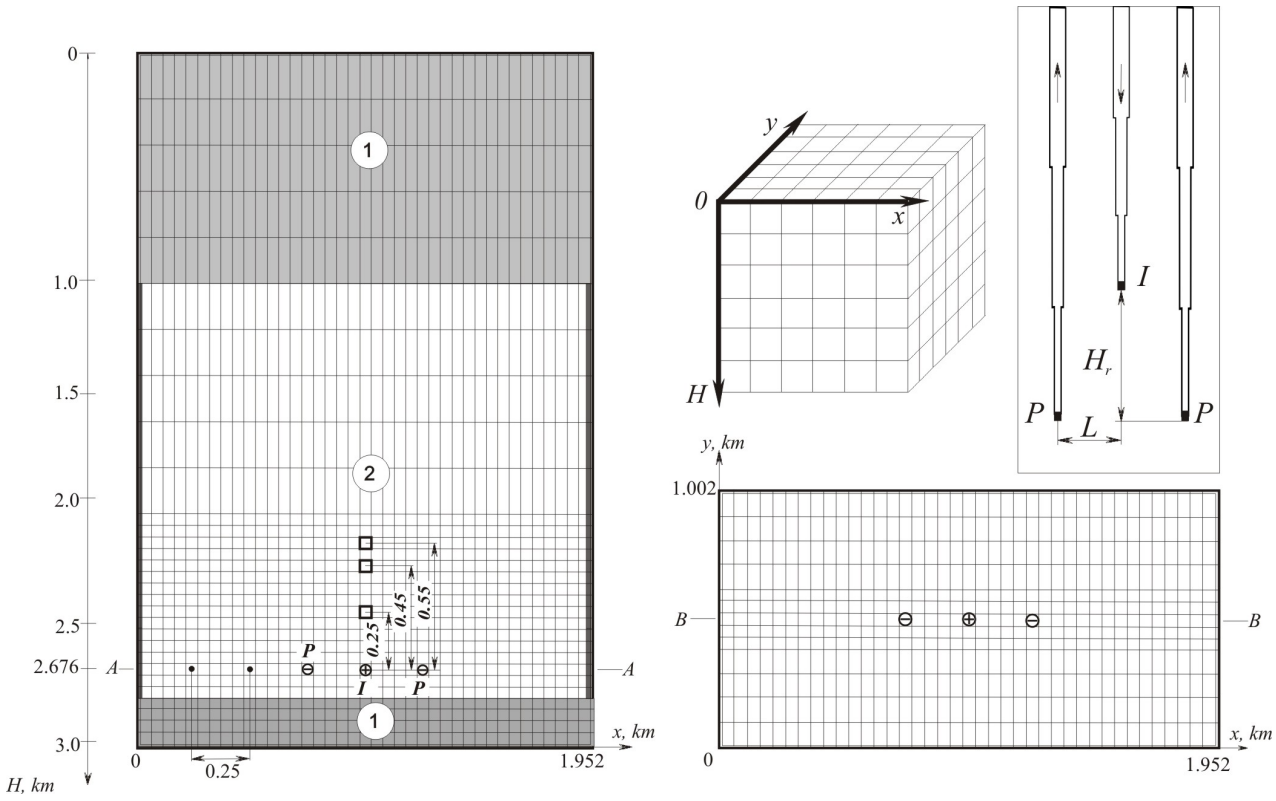

Figure 1: Triplet well pattern with computational grid. 1 – upper and lower regions of impermeable rocks; 2 – production permeable zone; *P* – producer; *I* – injector

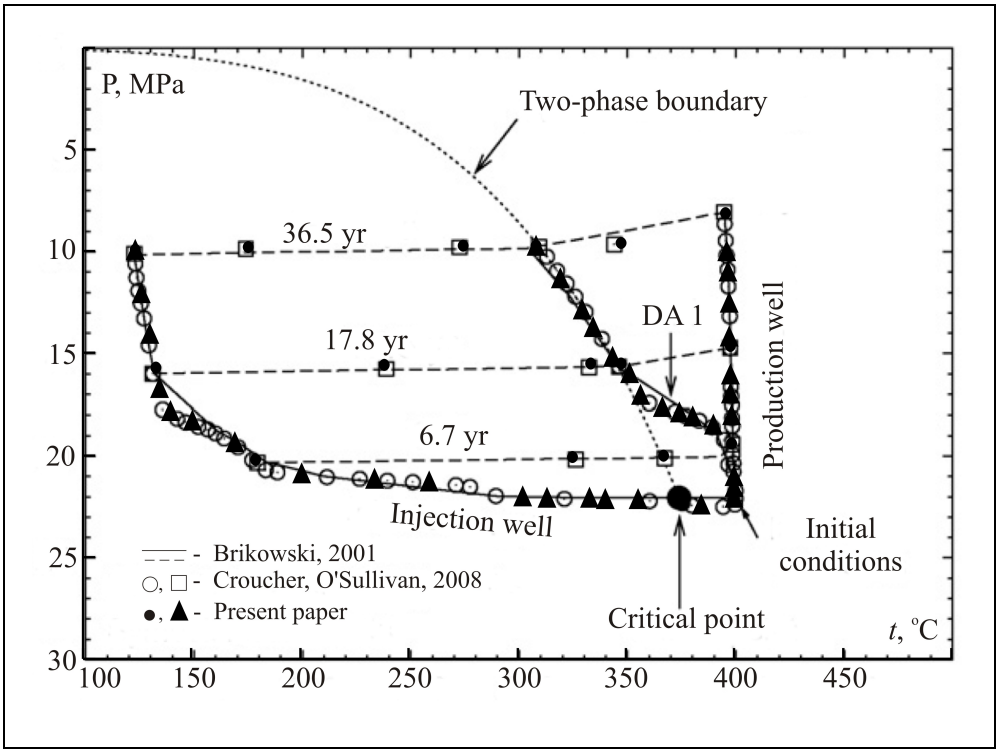

Figure 2: Pressure–temperature diagram for the modeled supercritical five-spot problem. Point DA 1 is at the midpoint between the injection and production wells

Thus, the selected geometry of simulated EGS is practically attainable. At the same time, the existence of naturally fractured rocks in the above range of depths is possible. For example, during the Cooper Basin project, drilling water saturated granites were found at a depth 4.5 km (Vörös, Weidler and Wyborn, 2007).

3. SIMULATION RESULTS

3.1 The Influence of *L* on the Circulating Fluid Parameters

The analysis of phase change during exploitation and determining its dependence on well pattern geometry (L and H_r) is important for the determination of rational parameters of supercritical EGS. In the case of "in-line" well arrangement (H_r=0 m and L = 500 m), a wet steam zone was predicted to form after one year of exploitation near the bottom of the producers as a result of fluid withdrawal and pressure decline. The volumetric water saturation S increased in the direction toward the producers from wet steam boundary, as depicted in Figure 3a.

In the other part of production zone, the fluid was supercritical, (i.e. S=0.5 in HYDROTHERM terms) (Hayba and Ingebritsen, 1994). In two years, the condensation front spread into a larger horizontal cross section of the zone. In five years, almost the entire cross section became filled with wet steam. The water saturation grew toward the bottom of the producers. A liquid water zone formed between the producers and the injector. In five years, the steam fraction declined further, and a ring-like liquid zone formed around the injector. The water pressure was greater than critical pressure in and around the injector bottom.

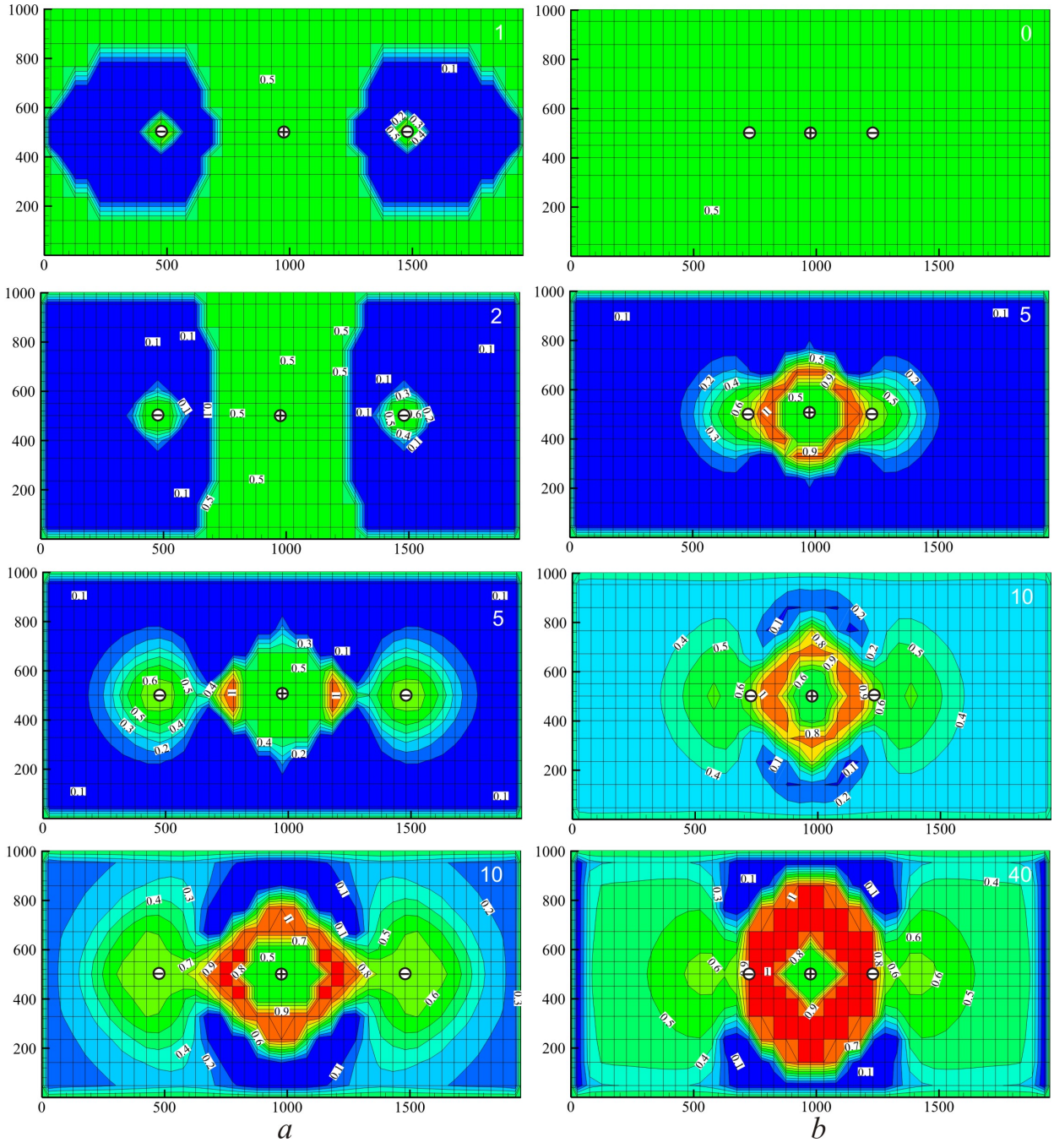

Figure 3: Volumetric water saturation changes in production zone during the exploitation with H_r=0 m, L = 500 m (*a*) and 250 m (*b*). The exploitation time (years) is shown in upper-right corner. The vertical axis is the width of the production zone (m), and the horizontal axis is a *x* value (m)

A superheated steam zone formed below and near the producer bottom and spread during exploitation to the boundaries of the production zone. When the distance between the producers and the injector was reduced (L = 250 and 200 m), the phase transition process had the same character, but its intensity and mean water saturation increased, as illustrated in Figure 3b. With fixed H_r, the distance L determines the parameters as follows: 1. width of the disturbed state of the production zone, 2. rate of rock cooling, 3. pressure, temperature and water saturation gradients near of the bottoms of the wells. At smaller L values, the rocks were cooled more, pressure became lower near the producer bottoms, and the width of the region with a considerable water saturation gradient became smaller.

3.2 The Influence of H_r on the Circulating Fluid Parameters

A greater value of H_r resulted in a wet steam production zone with a larger horizontal cross section, as shown in Figure 4. The fluid was in liquid phase in the vertical cross section down to a depth of 2600 m in the region near the production zone boundary. A decrease in water saturation occurred down to the same depth. The fluid existed in a wet steam phase, and nearly dry steam (S=0.1) was found in a layer with a thickness of 200 m. The layer was continuous along the x axis when the injector bottom is shallower than that of the producer. For the "in-line" case (H_r=0), the fluid was liquid in a narrow region between the injector and producers bottoms. Below a depth of 2.8 km, water saturation decreased, and wet steam became dry and then superheated. Finally, the fluid became supercritical.

The pressure declined near the producer and increased near the injector. The pressure significantly changes only in a production zone. The decompression front penetrated less than 50 m into the lower impermeable layer, as shown in Figure 4. The rock cooling front spread in the vicinity of producer and injector bottoms and did not penetrate the lower impermeable layer.

The temperature gradient was significantly larger in the rocks between the producers and the injector when H_r=0. When the injection rate was 15 kg/s and L=250 m, the well system worked stably for 30 years with a minimal heat load of 20 MW. When H_r=0 and L=250 m, full condensation occurred in the producer bottom after 20 years of exploitation. For larger H_r values (250, 450, 550 m) in the producer bottom, the steady pressure and enthalpy decreased and the fluid remained wet steam during the exploitation. When H_r was increased from 0 to 550 m, the steady value of the required injector bottom pressure decreased from 42 to 39 MPa.

3.3 The Influence of Injection Rate on the System Parameters

The rate of pressure and enthalpy decline increased with the injection rate. By the end of exploitation, the rate of growth of water saturation in the producer bottom and the rate of growth of required injection pressure increased as well, as shown in Figure 5. Injection rates of 5, 10 and 15 kg/s, resulted in the following steady producer bottom values: pressure — 19, 15, 8.5 MPa; temperature — 360, 340, 300^{o}C; enthalpy — 1900, 1700, 1400 kJ/kg; mass water saturation — 85, 92, 96 %; and required injection rate — 26, 34 and 43 MPa, respectively.

3.4 The Influence of L and H_r on the Extracted Thermal Energy

The extracted thermal energy Q can be calculated as follows:

$$Q = G\sum_{i=1}^{n}\left(h_{Pi} - h_{Ii}\right)\Delta t_i .$$

where G is the injector mass rate; h_{Pi}, and h_{Ii} are the mean fluid enthalpies at the producer and injector, respectively; Δt_i is the time interval of interest; $n=n(t)$ is the number of calculated time intervals by the end of exploitation time t. The mean enthalpies were calculated over an each time step of simulations.

<u>*Case with L=250 m.*</u> After five years of exploitation, the extracted heat was nearly equal for all values of H_r, as shown in Figure 6. In this initial exploitation period, the extracted heat is even larger than its value when H_r is zero as long as the injector bottom was higher than that of the producer. When H_r = 0 within an exploitation period of less than 30 years, the mean extracted heat was larger than that when H_r>0. After 37 years, the extracted heat was larger when H_r =250 m than when H_r=0, as shown in Figure 6. After 40 years, the difference between extracted heat for different H_r values is greater than 10%.

<u>*Case with L=500 m.*</u> Here, the dependence of extracted heat on H_r is inverse to the above case. When the depths of producers and injector were equal (H_r=0), the extracted heat was less than that when H_r>0, as shown in Figures 6 and 7. Finally, the extracted heat was less than that when L = 250 m for all H_r values.

CONCLUSION

The technological parameters of supercritical EGS were influenced by the well rate, production zone permeability, relative vertical distance between the bottoms of the injector and the producer, and distance between injector and producers. It is more rational to arrange well systems such that L=250 m and H_r=0, because parameters of producers are higher than when L=500 m, and required injection pressure is lower than when L=200 m.

ACKNOWLEDGEMENTS

The authors would like to thank Dr. P.A. Hsieh (USGS) for granting of the software HYDROTHERM version 2.2 for PC and Dr. S.E. Ingebritsen, Dr. D.O. Hayba and Dr. K.L. Kipp (USGS) for advising on the software and providing software documentation. The authors would like to thank the translator I.V. Maslovskaya (Scientific Research Geotechnological Center – RSGC, Far East Branch of Russian Academy of Science) for translating this paper in English.

REFERENCES

Brikowski, T.H.: Modeling supercritical systems with TOUGH2: preliminary results using EOS1SC equation of state module, *Proceedings* 26th Workshop on Geothermal Reservoir Engineering, Stanford, CA (2001).

Croucher, A.E., and O'Sullivan, M.J.: Application of the computer code TOUGH2 to the simulation of supercritical conditions in geothermal systems, *Geothermics*, **37,** (2008), 622–634.

Hayba, D.O., and Ingebritsen, S.E.: The computer model Hydrotherm, a three–dimensional finite–difference model to simulate ground–water flow and heat

transport in the temperature range of 0 to 1,200°C, *U.S.G.S. Water Res. Invest. Rep.*, (1994), 85 p.

Ledru, P., and Genter, A.: Enhanced Geothermal Innovative Network for Europe, *Proceedings*, European Geothermal Congress, (2007).

Kipp, K.L., Hsieh, Jr. P.A., and Charlton, S.R.: Guide to the revised ground-water flow and heat transport simulator: HYDROTHERM—Version 3, *U.S. Geological Survey Techniques and Methods*, (2008), 160 p.

Kissling, W.M., and White, S.P.: Supercritical TOUGH2–Code description and Validation, *Industrial Research Limited Report 905*, (1999).

Pritchett, J.W.: STAR: A geothermal reservoir simulation system, *Proceedings*, World Geothermal Congress, Florence, Italy, (1995), 2959-2963.

Pruess, K., Oldenburg, C., and Moridis, G.: TOUGH2 user's guide, version 2.0, *Report LBNL-43134*, Lawrence Berkeley National Laboratory, Berkeley, CA, USA, (1999), 209 p.

Sanyal, S.K., and Butler, S.J.: An analysis of power generation prospects from enhanced geothermal systems, *Geothermal Resources Council Transactions*, **29**, (2005).

The Future of Geothermal Energy - Impact of Enhanced Geothermal Systems (EGS) on the United States in the 21st Century, 2006. *MIT-led interdisciplinary panel*, Massachusetts Institute of Technology, USA, (2006).

Vörös, R., Weidler, R., and Wyborn, D.: Thermal modeling of long term circulation of multi-well development at the Cooper Basin hot fractured rock (HFR) project and current proposed scale-up program, *Proceedings*, 32th Workshop on Geothermal Reservoir Engineering Stanford, CA (2007), 339-345.

Watanabe, K., Niibori, Y., and Hashida, T.: Numerical study on heat extraction from supercritical geothermal reservoir, *Proceedings*, World Geothermal Congress, (2000), 3957-3961.

Yano, Y., and Ishido, T.: Numerical investigation of production behavior of deep geothermal reservoirs at supercritical conditions, *Geothermics*, **27**, (1998), 705–721.

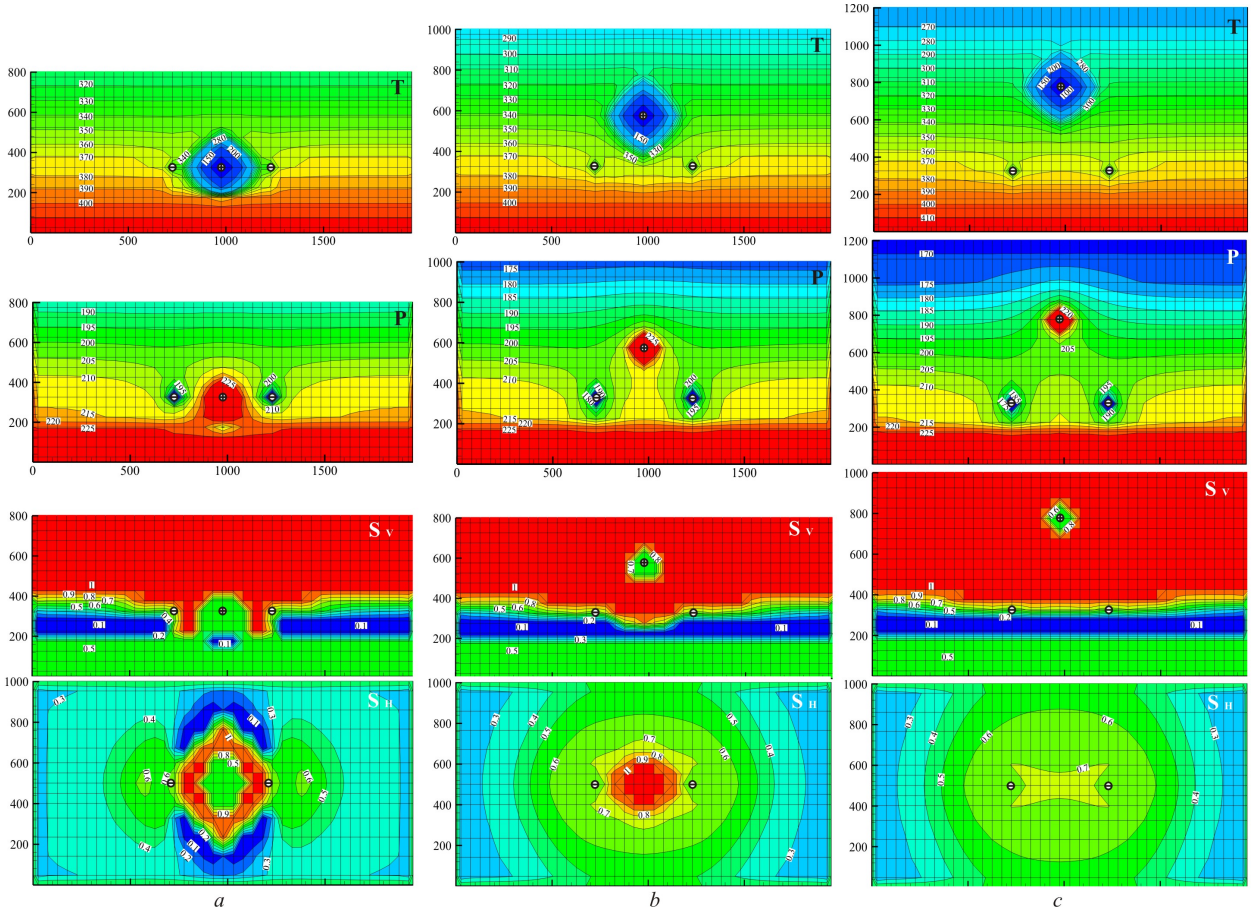

Figure 4: The distribution of production zone parameters after 10 years of exploitation at different H_r values (m): *a* – 0; *b* – 250; *c* – 450. T, P, and S_V are temperature (°C), pressure (bar) and water saturation in a vertical cross section *B*-*B*. S_H – water saturation in a horizontal cross section *A*-*A*. The vertical axis is the height (m) from the model bottom (*H*=3 km), and the horizontal axis is an *x* value (m). For S_H, the vertical axis is the width (m) of production zone along the *y*-axis

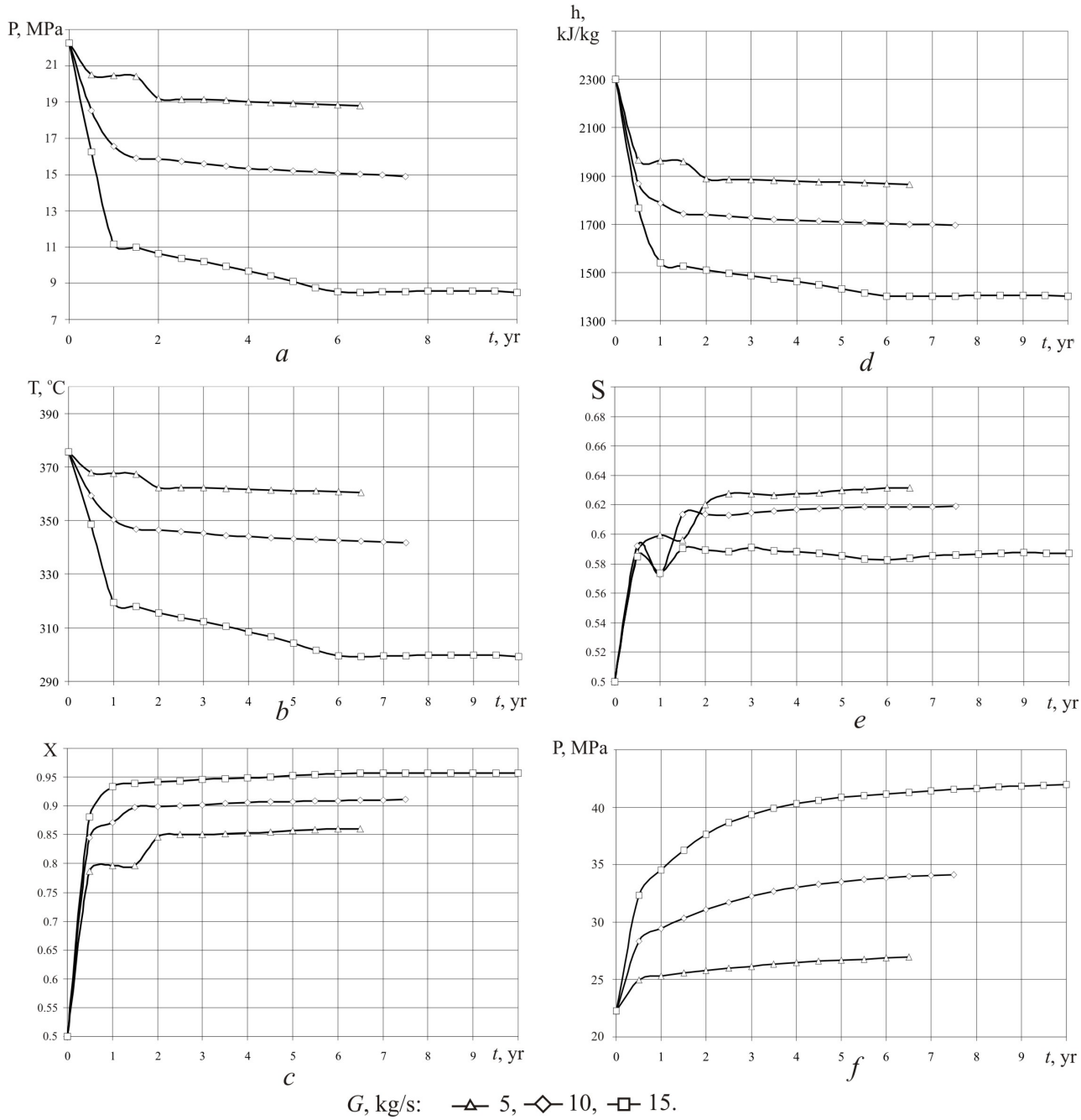

Figure 5: Calculated pressure (*a*), enthalpy (*d*), temperature (*b*), mass and volume water saturation (*c*, *e*) in producer and pressure (*f*) in injector bottom for different injection rates

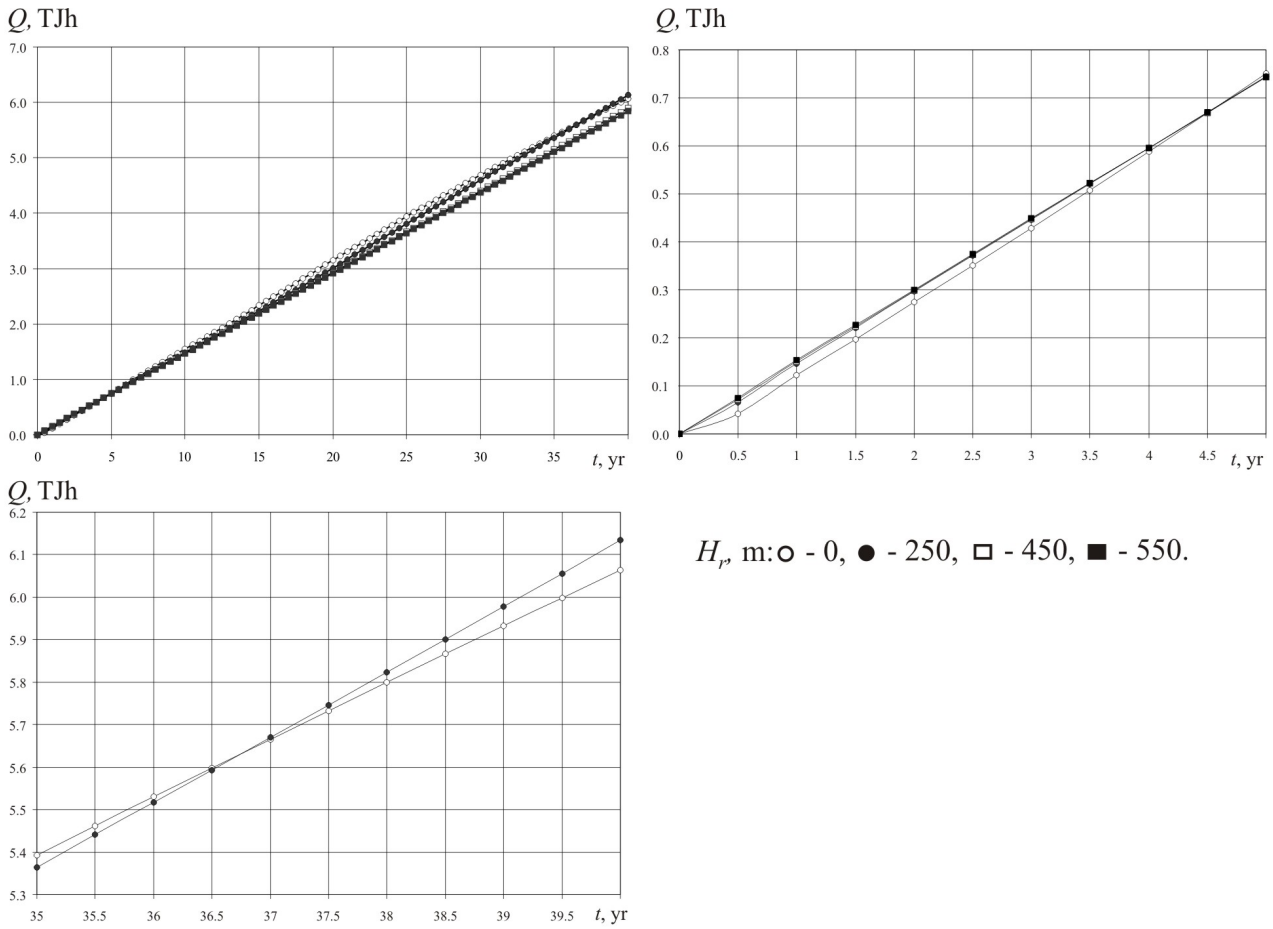

Figure 6: The dependence of extracted thermal energy from production zone rocks during exploitation on H_r when L=250 m

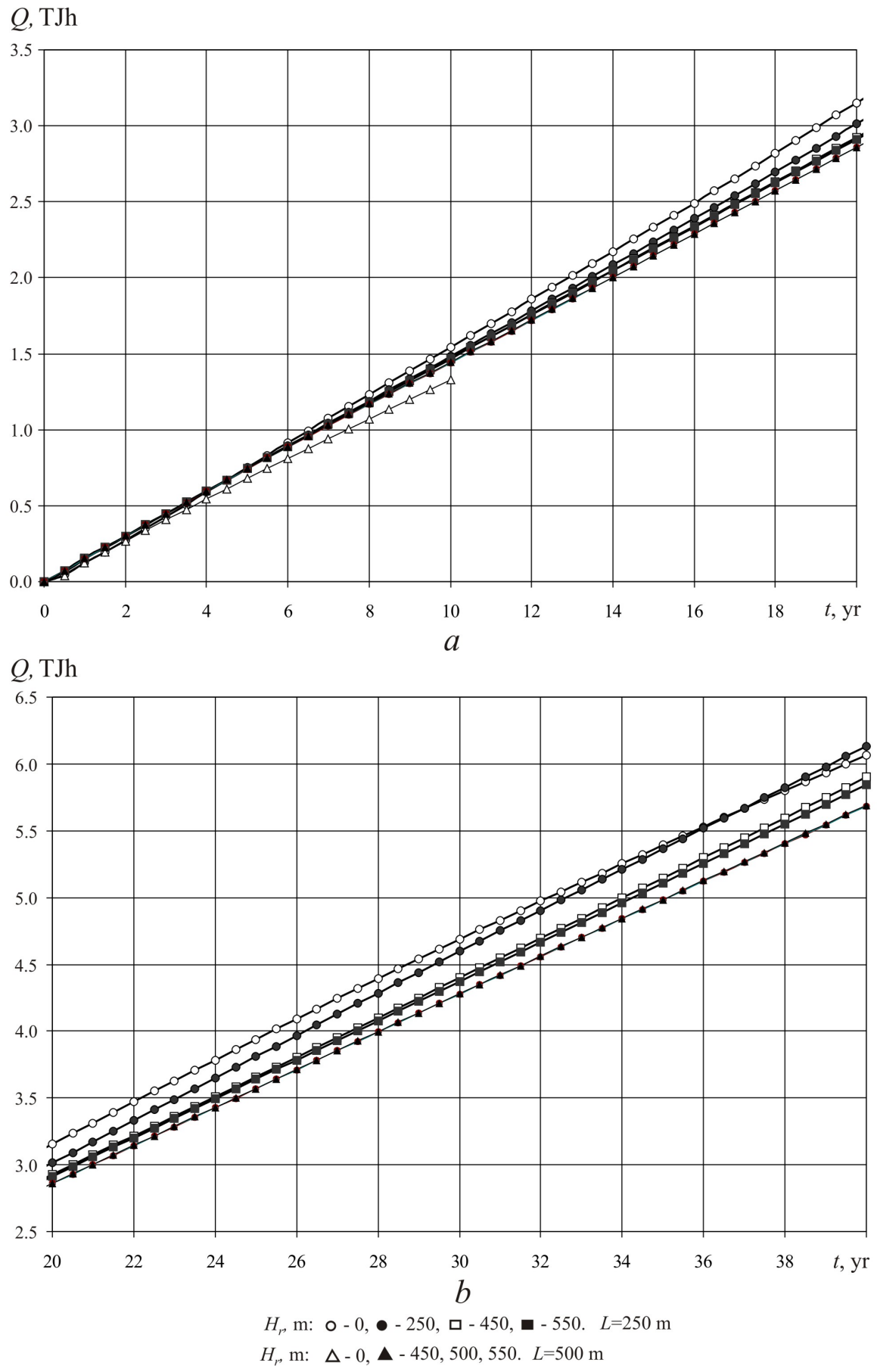

Figure 7: The dependence of extracted thermal energy from production zone rocks during exploitation on *L* and H_r